Mutual ionization in 200-keV H^-+He collisions

T. Ferger,[1] D. Fischer,[1] M. Schulz,[2,3] R. Moshammer,[1] A. B. Voitkiv,[1] B. Najjari,[1] and J. Ullrich[1]
[1]*Max-Planck-Institut für Kernphysik, Saupfercheckweg 1, 69117 Heidelberg, Germany*
[2]*Department of Physics and Laboratory for Atomic, Molecular, and Optical Research, University of Missouri-Rolla, Rolla, Missouri, 65409, USA*
[3]*Institut für Kernphysik, Universität Frankfurt, Max-von-Laue-Strasse 1, 60438 Frankfurt, Germany*
(Received 5 July 2005; published 19 December 2005)

We studied mutual ionization in 200-keV H^-+He collisions in a kinematically complete experiment by measuring the fully momentum-analyzed recoil ions and both active electrons in coincidence. Comparison of the data to our calculations, based on various theoretical models, show that mutual ionization proceeds predominantly through the interaction between both electrons. The post-collision interaction between the outgoing ejected electrons as well as higher order processes involving the interaction between the core of both collision partners are also important.

DOI: 10.1103/PhysRevA.72.062709 PACS number(s): 34.50.Fa, 34.10.+x

INTRODUCTION

The last decade has seen rapid progress in experimental studies of ionization of light targets by swift ion impact. Apart from early experiments at very low ion energies (e.g., Ref. [1]), in previous years measurements were mostly restricted to total cross sections [2,3] and cross sections differential in ejected electron parameters [4,5]. Cross sections differential in projectile parameters are much more difficult to measure because the scattering angles and energy losses are usually of the order of or even smaller than the experimental resolution (i.e., the divergence and energy spread of the ion beam). In fact, for fast heavy projectiles both quantities are immeasurably small even using cold beams in ion cooler-storage rings. As a result, even for proton impact the first measured singly differential cross sections at large collision energies as a function of the projectile scattering angle were only obtained in the late 1980s [6]. It took almost another 10 years before the first doubly differential cross sections (in solid angle and energy loss of the projectile) were reported [7,8].

A major breakthrough, enabling much more detailed studies of ionization processes by ion impact, was achieved with the development of recoil-ion momentum spectroscopy [3,9,10]. The cross sections as a function of the various recoil-ion momenta provided valuable and complementary information to those obtained from electron spectra on the collision dynamics (see e.g., Ref. [11]). More importantly, by measuring the momentum-analyzed recoil-ions and electrons in coincidence and deducing the scattered projectile momentum from the conservation laws, kinematically complete experiments on single ionization became possible, essentially independently of the projectile mass and velocity [12]. The first measured fully differential single ionization cross sections (FDCS) for ion impact were only reported a few years ago [13]. Since then, a large amount of data in hitherto unexplored kinematical regimes on FDCS for single ionization of He by ion impact has been generated [14–23].

The theoretical description of single ionization proved to be much more problematic than was assumed prior to these FDCS measurements. Especially the continuum distorted wave-eikonal initial state (CDW-EIS) model was very successful in predicting measured doubly differential electron spectra even for very large perturbation η (projectile charge to velocity ratio Q_p/v_p) [24], where the calculations become increasingly difficult. However, the same model failed dramatically in describing electron spectra as a function of the projectile deflection [25] and, even more severely, the FDCS for the same collision system (3.6 MeV/amu Au^{53+}+He) [15]. Most surprisingly, significant discrepancies were found between experiment and theory in the FDCS for very small η [14], where even the first Born approximation (FBA) was expected to provide an adequate description. For electrons emitted into the scattering plane (defined by the initial and scattered projectile momenta) the agreement was very good, but outside the scattering plane large qualitative and quantitative discrepancies were observed. Although several theoretical attempts have been made to interpret these differences between theory and experiment [26,27], no major progress has been achieved until the present day.

By now a lot of experimental data on FDCS for single ionization exist covering a broad range of different collision systems and a broad regime of perturbations from η=0.1 to η=4.4 (in a.u., a value given in a.u. is measured relative to the corresponding value of an electron in the ground state of H). At this stage it therefore seems reasonable to turn to somewhat more complex (but not too complicated) ionization processes and to fully exploit the opportunities provided by heavy particle projectiles compared to electrons, in order to advance our understanding of collision-induced few-particle quantum dynamics. One fundamental step forward is to study double ionization of the target atom, where electron-electron correlations must be taken into account. Here, some nearly fully differential data already exist [28,29]. Another important step is to investigate mutual ionization of both collision partners, whereby two-center effects can be studied. Although this process is more complicated than double ionization in that it requires a structured projectile, one important advantage is that the mutual ionization can proceed through a single interaction (between the two electrons to be

ionized), while double ionization requires at least two interactions. In that sense mutual ionization is the more simple process.

For mutual ionization, like in the case of pure target ionization, multiple differential data became only available quite recently [30,31], following numerous experimental and theoretical total cross section studies (see references in Refs. [30,31]). First angular distributions for electrons ejected into the scattering plane were reported a few years ago for 3.6 MeV/amu C^{2+}+He collisions [32]. As in the earlier investigations mentioned above, the most important question which was addressed in that work was to what extent the mutual ionization process proceeds through the interaction between the two active electrons and to what extent this particular reaction channel can be separated from other mutual ionization mechanisms. Since the reaction channel involving the electron-electron interaction constitutes a first-order process, as mentioned above, one might expect it to be more important than a second-order mechanism in which both electrons are ionized independently by an interaction with the core of the other collision partner. Indeed, a pronounced angular correlation between both ejected electrons, demonstrating a strong interaction between them, was observed in certain kinematical regimes. In other regimes, the angular correlation between the electron ejected by one collision partner and the core of the other partner, which is indicative for the second-order process mentioned above, was more pronounced. Furthermore, the angular distributions of the electrons ejected from the ionic projectile into the scattering plane in such an $(e,2e)$-like process revealed the typical features routinely observed in the FDCS for single ionization of light atoms by free electron impact, although the data were integrated over all electron energies and momentum transfers.

In the work presented in this paper, we have advanced multiple differential studies on mutual ionization to a collision system, namely 200-keV H^-+He, which should behave quite differently from the one investigated in Ref. [32] in several aspects. First, the binding energy of the projectile electron is much smaller (0.7 eV compared to 48 eV in C^{2+}). Thus, it is expected that we systematically approach a situation characteristic for free electron impact. Second, in a mutual ionization process the projectile becomes neutralized. Therefore, one might expect that both electrons get ejected without being affected by any post-collision interaction (PCI) with the outgoing projectile. On the other hand, one cannot rule out the possibility that the ejected electrons are mostly affected by a PCI with only one of the charged particles which initially were constituents of the H^- ion. Then the question is whether the data will show the characteristics of the attractive PCI between the projectile nucleus and the target electron or of the repulsive PCI between both ejected electrons. Third, since the perturbation is roughly twice as large ($\eta=0.35$) as in the previous experiment, higher-order effects should be significantly more important and can be explored in detail. All of these aspects are addressed in this work.

EXPERIMENT

The experiment was performed at the Max-Planck-Institut für Kernphysik in Heidelberg. An H^- beam was generated with a Duoplasmatron ion source and accelerated to 200 keV. The projectile beam was crossed with a very cold ($T<1$ K) neutral He beam from a supersonic gas jet with a density of about 10^{11} atoms/cm^2. The projectiles which were neutralized in the collision (and which were selected by deflecting the charged beam components out using a magnet) were detected by a channel plate detector. The recoil ions and the ionized electrons were extracted in the longitudinal direction (defined by the initial projectile direction) by a weak electric field of 2.3 V/cm. A uniform magnetic field of 20 G confined the transverse motion of the electrons so that all electrons with a transverse momentum of less than 3 a.u. were guided onto the detector. The momentum vectors of the recoil ions and the ejected electrons as well as the recoil ion charge state were determined by using position sensitive detectors and time-of-flight techniques, where a fast signal from the projectile detector served as a timing reference. The momentum resolutions depend on the momenta themselves and therefore averaged values are provided. In the longitudinal direction, defined by the projectile beam axis (z direction), they are 0.2 a.u. and 0.1 a.u. for the recoil ion and for the electrons, respectively. In the direction of the jet expansion (y direction), the corresponding numbers are 0.3 a.u. and 0.2 a.u. and for the x direction 0.2 a.u. and 0.1, respectively (in all cases the full width at half-maximum, FWHM, is provided).

For each mutual ionization event both electrons were detected simultaneously with a single detector employing a multihit technique (deadtime $\approx$10 ns). It should be noted that since one electron is emitted from the moving projectile frame and one from the target frame at rest, their time of flight is in most cases very different. As a result, losses due to the multihit-deadtime are not as critical as in double ionization experiments using this method. The momentum of the neutralized projectiles was determined from momentum conservation. From the electron momenta it is straightforward to calculate the emission angles.

THEORY

In order to describe the H^--He collisions we use the first Born approximation (FBA) in the projectile-target interaction. Both the projectile and the target are assumed to have just one active electron. Since the FBA is a first-order treatment, here mutual ionization can only proceed through an interaction between these active electrons. The initial and final states of the active electron in helium are obtained by solving numerically the Schrödinger equation for a spherically symmetric Hartree-Fock potential. The initial and final states of the active electron in H^- were found by solving the Schrödinger equation for a Yukawa-type potential used to model the short-range force experienced by the active electron in H^-, which is a common approach to model H^- [33]. In addition, in order to get some insight into how the short-range nature of the binding force in H^- can influence the collision process we also performed calculations in which the H^- was replaced by a hydrogenlike ion with an effective nuclear charge of 0.235 a.u. which has the ground state energy equal to the binding energy of H^-.

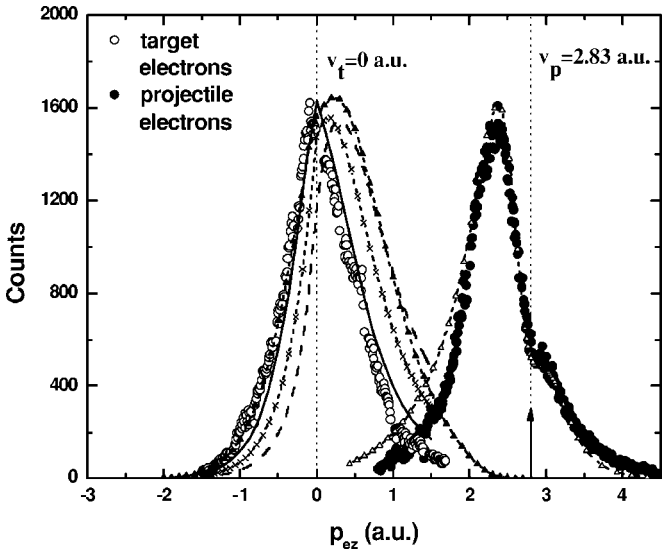

FIG. 1. Longitudinal electron momentum spectra for the target electrons (open symbols) and projectile electrons (closed symbols). The arrow indicates the projectile speed v_p. Triangle-dashed curves, FBA for mutual ionization with Yukawa potential for H^-; solid curve, CDW-EIS for pure target ionization by antiproton impact; cross-dashed curve, FBA for pure target ionization by proton impact; dashed curve, CDW-EIS for pure target ionization by proton impact.

Besides the first order consideration, briefly discussed above, the longitudinal spectrum of electrons emitted from helium in collisions with H^- was considered using the continuum distorted wave-eikonal initial state (CDW-EIS) approximation [34]. This was done by assuming that this spectrum (which is obtained for mutual ionization events) is similar to that produced in single ionization of helium by antiprotons having the same collision velocity as the H^- ions. In the CDW-EIS approach the final state of the colliding (effective) three-body system is approximated by a product of three two-body Coulomb wave functions. The initial state is also represented by a product of three two-body states in which, however, the actual Coulomb wave functions for the corresponding two-body continuum states are replaced by their asymptotic (eikonal) form. Higher-order effects are accounted for in both the initial and final state. In particular, effects due to PCI, which we will discuss in some detail in the next section, are included in our CDW-EIS calculations.

RESULTS AND DISCUSSION

Longitudinal electron momentum spectra

We start the presentation of the results by analyzing the longitudinal electron momentum spectra. These are shown for the target electrons (open symbols) and projectile electrons (closed symbols) in Fig. 1. It should be noted that in the experiment we cannot really distinguish from which collision partner an electron was ejected. For simplicity, we refer to the slower (faster) electron as the target (projectile) electron. Inspecting the spectrum for the target electrons, we note a striking similarity to those obtained for pure target ionization by highly charged ion impact (like, e.g., 3.6 MeV/amu Se^{28+}, 100 MeV/amu C^{6+}, or 1 GeV/amu U^{92+}) [35–37]. In particular, we find a pronounced cusp shape peaked approximately at $p_{e_z}=0$. Furthermore, a forward-backward asymmetry is seen, i.e., the positive-momenta wing of the peak extends to larger momenta than the negative-momenta wing. Such a shape is quite characteristic for ionization by fast highly charged ion impact, where it is usually explained in terms of an attractive PCI. It is therefore tempting to interpret the present spectrum by a PCI between the projectile nucleus and the outgoing target electron. However, an analysis of theoretical spectra, which we will present in the following, leads to a completely different conclusion.

The triangle-dashed curve in Fig. 1 shows our FBA calculation on mutual ionization in which the H^- projectile is described by the Yukawa potential (FBA-Y). The cross sections are presented in arbitrary units and all calculations are normalized to approximately match the magnitude of the data in the maxima. Large discrepancies to the experimental data are quite obvious. In particular, the results of the calculation are significantly shifted in the forward direction compared to the data. However, this shift is not due to any PCI with the projectile since this calculation represents a first-order treatment. Rather, the shift can be explained by the relatively large longitudinal component of the momentum transfer q_z, which is approximately given by $q_z=\Delta E_p/v_p$ (where ΔE_p and v_p are the projectile energy loss and velocity, respectively). Since in a first-order treatment the electrons roughly follow the momentum transfer, this relatively large positive value of q_z is also reflected in the longitudinal electron spectra.

In contrast, the CDW-EIS calculation for pure target ionization, where the H^- projectile is treated as an antiproton (solid curve in Fig. 1), reproduces the cusp shape and the forward-backward asymmetry observed in the data very well. However, here again, this shape cannot be explained by an attractive PCI because there is no positively charged constituent in the projectile. Instead it appears that it can be described in terms of a combination of the above described forward shift due to the relatively large q_z and a backward shift due to a repulsive PCI with the antiproton projectile. To illustrate this, we also show in Fig. 1 the FBA for pure target ionization (cross-dashed curve) and a CDW-EIS calculation (dashed curve), both for proton impact. Qualitatively, the FBA calculation looks very similar to the FBA-Y results for mutual ionization, except that the forward shift relative to the data is somewhat smaller. In contrast, the CDW-EIS calculation for proton impact is shifted even more in the forward direction, which is due to the attractive PCI with a positively charged proton projectile. In the CDW-EIS calculation for antiproton, on the other hand, the repulsive PCI counteracts the forward shift due to q_z. The present analysis therefore provides strong evidence that in the data the repulsive PCI with the projectile electrons (in the calculation modeled as an antiproton projectile) is not compensated by the attractive PCI with the projectile nucleus, although the projectile got neutralized in the collision.

For the projectile electrons, we observe a more complex structure in the longitudinal momentum spectrum. Apart

from the main peak at about 2.3 a.u., we also find a "bump" which starts approximately at the projectile velocity $v_p = 2.83$ a.u. (indicated by the arrow in Fig. 1). It should be noted that the uncertainty in the calibration gets larger with increasing longitudinal momentum p_{e_z} and reaches about 0.1 a.u. at $p_{e_z} = v_p$. If the mutual ionization proceeds predominantly by the electron-electron interaction, the energy to overcome the initial binding of both electrons must be provided by the projectile electron (in the target rest frame). In this first-order process, the total ionization potential of both electrons (25.3 eV) therefore leads to a change in the longitudinal projectile electron momentum from initially 2.83 a.u. to at least 2.48 a.u., which is consistent with the location of the main peak. It is then tempting, but, as we will show below, premature, to associate the "bump" with a higher-order process in which each electron is ejected due to an interaction with the core of the other collision partner. There, the energy to overcome the ionization potential is provided by the H^0 core and the longitudinal projectile electron momentum spectrum (dominated by low-energy electrons in the projectile frame) should be peaked approximately at v_p. Again, our theoretical analysis leads to a different conclusion.

The triangle-dashed curve shows our FBA-Y calculation for mutual ionization. Although the small-momentum wing of the main peak is overestimated, overall the data are qualitatively well reproduced. Most importantly, the "bump" near v_p is very well described. In this model, the mutual ionization process can only proceed through the electron-electron interaction. Therefore, the comparison between the data and the FBA-Y strongly suggests that the "bump" is not due to the higher-order process discussed above.

In order to understand the origin of the "bump" in the FBA-Y calculation it is helpful to analyze the calculated energy spectrum of the projectile electrons in the projectile frame, which is shown in Fig. 2. The solid curve is an FBA calculation for H-like projectiles (FBA-H) and the dashed curve shows the FBA-Y results. Both models show a strong minimum at an electron energy $E_e = 0$, which is much more pronounced in the FBA-Y calculation. For the target ionization, in contrast, the energy spectrum (not shown in Fig. 2) is almost flat near $E_e = 0$ and continuously drops thereafter. Two factors contribute to this minimum, first, in the FBA-H as well as the FBA-Y calculation the projectile electron must provide a minimum longitudinal momentum transfer in order to overcome the ionization potential of both electrons. In the projectile frame, this means that the electron is accelerated from rest to some minimum velocity, i.e., energies around $E_e = 0$ are suppressed. Second, in the FBA-Y an additional suppression of $E_e \approx 0$ occurs due to the short-range nature of the Yukawa potential. For systems bound by a long-range Coulomb potential, $d\sigma/dE_e$ approaches a constant limit as E_e goes to zero. In contrast, for systems bound by a short-range potential $d\sigma/dE_e \sim E_e^{1/2+l}$ $(l = 0, 1, \ldots)$ leading to a minimum in the energy spectrum at $E_e = 0$. An energy $E_e = 0$ in the projectile frame corresponds to an electron speed equal to v_p in the target frame. The "bump" in the longitudinal projectile electron momentum spectrum near v_p can therefore be explained by a suppression of the cross sections at v_p rather than by an enhancement above v_p.

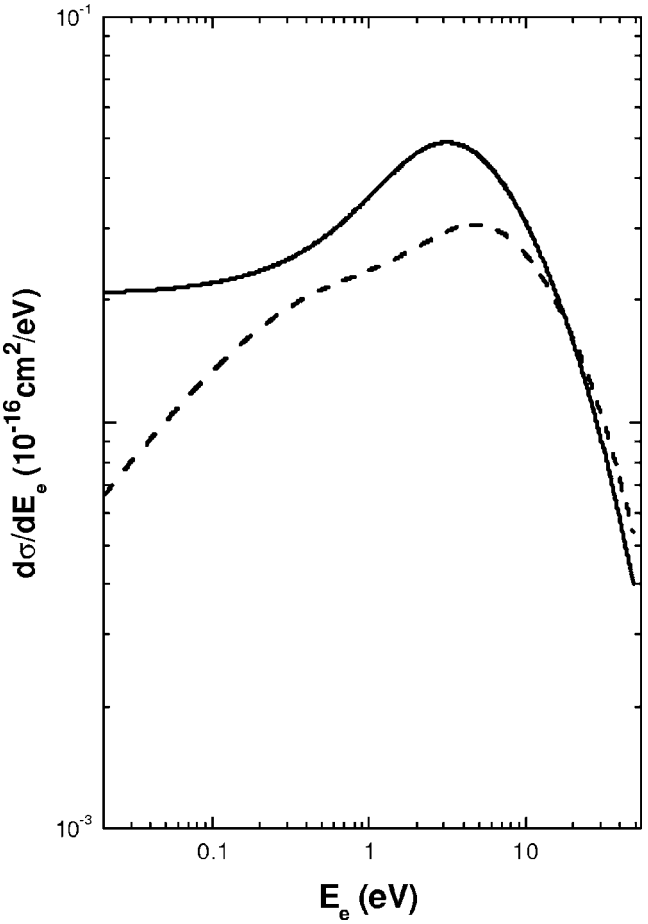

FIG. 2. Energy spectrum of the ejected projectile electrons in the projectile rest frame calculated with the FBA for H-like ion impact (solid curve) and with the FBA describing H^- by a Yukawa potential (dashed curve).

The reasonable agreement of the FBA-Y calculation with the experimental longitudinal projectile electron momentum spectrum suggests that here PCI effects are not very important, in contrast to the target electron spectrum. A possible explanation for this "broken symmetry" between the projectile and target ionization is the different charge states of the outgoing residual heavy collision partners. If the ejected target electrons are affected by a PCI with the ejected projectile electrons, the same PCI must also be acting on the ejected projectile electrons. However, the projectile electrons are also subject to a PCI with the positively charged residual recoil ion, which may to a large extent counteract the PCI with the ejected target electron. In contrast, the residual projectile is neutral after the mutual ionization process so that a corresponding compensation of the electron-electron PCI may not occur for the ejected target electrons. A more complete description of the projectile electron spectra would have to account for both types of PCI simultaneously. However, this would require at least a four-body treatment (two ejected electrons and the two residual heavy particles) using realistic potentials for both collision partners (e.g., Hartree-Fock for the target and Yukawa for the projectile), which is currently not feasible.

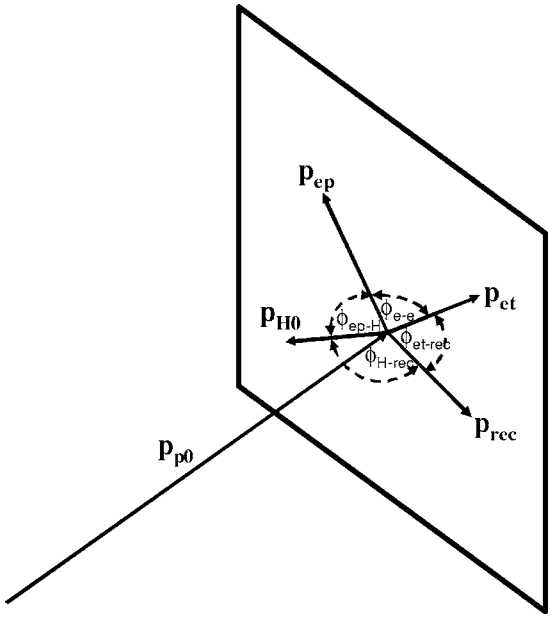

FIG. 3. Schematic sketch of the collision geometry. The rectangle indicates the azimuthal plane, which is the plane perpendicular to the initial H^- projectile momentum p_{p_0}. The other arrows indicate the momentum vectors of the various collision fragments projected into the azimuthal plane. Some of the angles plotted in Figs. 4–6 are shown.

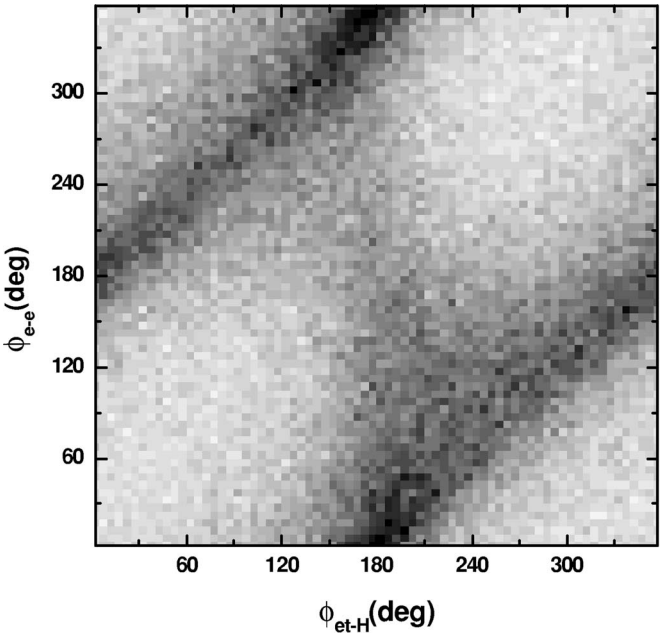

FIG. 4. The angle between both ejected electrons $\phi_{e\text{-}e}$ versus the angle between the target electron and the H^0 core of the projectile $\phi_{e_t\text{-}H}$ in the azimuthal plane.

In summarizing the longitudinal electron momentum spectra we ascertain that especially the projectile electron spectrum suggest that the mutual ionization proceeding through the electron-electron interaction dominates over the higher-order process in which each electron is ejected by an interaction with the core of the other collision partner. However, this does not mean that higher-order contributions are generally unimportant. On the contrary, the target electron spectrum can only be reproduced if the repulsive PCI with the projectile electron is accounted for, i.e., higher-order effects in the electron-electron interaction are important. Nevertheless, it is remarkable how much detail, especially in the projectile electron spectrum, is readily reproduced by a first-order calculation.

Angular distributions in the azimuthal plane

In order to investigate the dynamics of mutual ionization in the transverse direction, i.e., in the plane perpendicular to the beam axis, we analyzed the azimuthal angular distributions of the various particles involved in the collision, which is illustrated in Fig. 3. The arrows indicated in the azimuthal plane, which is the plane perpendicular to the initial H^- projectile momentum vector, are the projections of the final-state momentum vectors of the various collision fragments into that plane. In Fig. 4 the angle between both ejected electrons $\phi_{e\text{-}e}$ (here and in the following all angles refer to the projections of the momentum vectors shown in Fig. 3) is plotted versus the angle between the target electron and the H^0 core of the projectile $\phi_{e_t\text{-}H}$. Earlier, Kollmus *et al.* [32] demonstrated that for fast positively charged ion impact the first-order mechanism proceeding through the electron-electron interaction leads to a 180° peak in $\phi_{e\text{-}e}$, nearly independent of $\phi_{e_t\text{-}H}$ (i.e., to a horizontal line in Fig. 4). Likewise, the mechanism proceeding through an interaction of each electron with the core of the other collision partner leads to a vertical line. Neither of these lines is observed in the present case. Instead we find the intensity accumulating along lines oriented at an angle of 45° relative to each axis, for which $\phi_{e\text{-}e}$-$\phi_{e_t\text{-}H}$=180°. Essentially the same behavior is found if $\phi_{e_t\text{-}H}$ is replaced by the angle between the projectile electron and the recoil ion $\phi_{e_p\text{-rec}}$.

From geometry it can be seen that $\phi_{e\text{-}e}$-$\phi_{e_t\text{-}H}$=180° is equivalent to $\phi_{e_p\text{-}H}$=180°, where $\phi_{e_p\text{-}H}$ is the angle between the projectile electron and the H^0 core. Likewise, the angle between the target electron and the recoil ion $\phi_{e_t\text{-rec}}$ has a maximum at 180°. Indeed, if $\phi_{e\text{-}e}$ is plotted versus $\phi_{e_t\text{-rec}}$ [Fig. 5(a)] or versus $\phi_{e_p\text{-}H}$ [Fig. 5(b)], respectively, strong maxima in $\phi_{e_t\text{-rec}}$ and especially in $\phi_{e_p\text{-}H}$ at 180° are observed. This shows that the internal correlation between each electron and its respective parent atom is stronger than the correlation between the two electrons or between each electron and the core of the other collision partner.

Applying the analysis of Kollmus *et al.* [32] to Figs. 4 and 5 it is not immediately clear whether these plots support the conclusion drawn from the longitudinal spectra that mutual ionization proceeds predominantly through the electron-electron interaction. In order to address this question in more detail, in Figs. 5(c) and 5(d) the theoretical counterparts of Figs. 5(a) and 5(b) are shown. These plots are calculated using the FBA-Y model. In the case of the target electrons [Figs. 5(a) and 5(c)], the qualitative agreement between experiment and theory is amazingly good. This shows that in spite of the lack of a horizontal line the data of Fig. 4 are

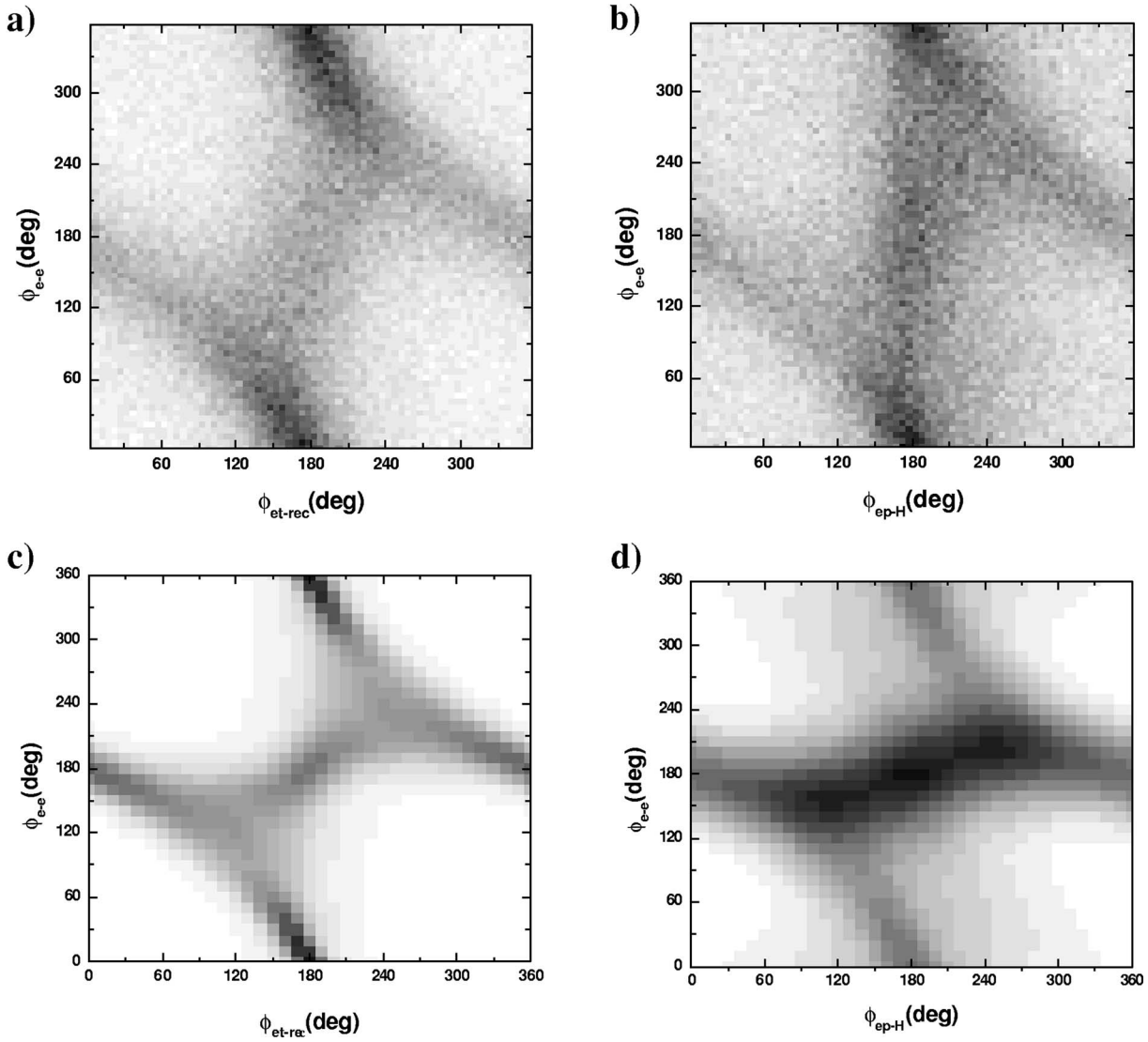

FIG. 5. The angle between both ejected electrons $\phi_{e\text{-}e}$ versus the angle between the target electron and the He^+ recoil ion $\phi_{e_t\text{-rec}}$ [panel (a)] and versus the angle between the projectile electron and the projectile core $\phi_{e_p\text{-}H}$ [panel (b)] in the azimuthal plane. Panels (c) and (d) show the corresponding theoretical spectra calculated with the FBA using the Yukawa potential for H^-.

consistent with the electron-electron interaction predominantly leading to mutual ionization. Furthermore, for the target electrons these cross sections are apparently not very strongly affected by higher-order effects, which are quite important to qualitatively describe the longitudinal momentum spectrum of the target electrons.

The pattern observed in Fig. 5(a) can now be explained in terms of a three-body correlation between the two ejected electrons and the residual He^+ ion. The correlation between the target electron and the He^+ ion originates already from the initial state. Since the entire target atom is initially at rest, at any given instant the electron momentum in the ground state must be compensated by the He^+ momentum, i.e., they always move back-to-back. The correlation between the two electrons is due to the mutual ionization process through the electron-electron interaction, in which some momentum q_e is exchanged between the electrons. If their momentum in the initial bound states p_{e_0} is small compared to q_e, after this interaction the electrons must move apart under a mutual angle of 180°. If, on the other hand, $q_e \ll p_{e_0}$ then the initial state correlation between the target electron and the recoil ion survives leading to a 180° peak in $\phi_{e_t\text{-rec}}$. Figure 5(a) suggests that mutual ionization is dominated by relatively small q_e.

For the projectile electrons the agreement between theory and experiment is much worse. While the data are dominated by a nearly vertical line at $\phi_{e_p\text{-}H}=180°$ in the calculation most of the intensity accumulates along a nearly horizontal line at $\phi_{e\text{-}e}=180°$. It appears that in the data the internal correlation in H^- is at least as important as in He while in the calculation the correlation in He is much stronger. Furthermore, the calculation seems to underestimate the internal correlation in the H^- projectile relative to the correlation between the two ejected electrons. The comparison between the data for the projectile and target electrons is surprising because the ionization potential for H^- (0.7 eV) is much smaller than for He (24.6 eV). Intuitively, one might therefore expect the Compton profile in He to be significantly

broader than in H^-. Therefore, the condition for a stronger internal correlation ($p_{e_0} > q_e$) should be easier to satisfy for He.

This comparison between the projectile and target electrons is currently not fully understood, however, there are some factors which may provide qualitative explanations. First, the Compton profile for H^- is not as narrow as suggested by the ionization potential. It should be kept in mind that the electrons of the ground state are indistinguishable. Therefore, for an estimate of the width of the Compton profile the average binding energy per electron is more relevant than the ionization potential, which is for H^- only a factor 5 smaller than for He (compared to a factor 30 for the ionization potentials) [38]. As a result, the Compton profile of H^- is only by about a factor of 2.4 narrower than the one of He. It is underestimated by our calculation because it models the H^- projectile as a one-electron system with a binding energy of 0.75 eV (instead of an average binding energy of 7.2 eV). Furthermore, a test calculation, using a Yukawa potential corresponding to a binding energy of 7.2 eV, shows that the visible signatures of the internal correlation in H^- not only become stronger with increasing binding energy in the projectile, but at the same time the apparent internal correlation in He becomes weaker. This can be understood as follows: the larger binding energy in H^- means that in the projectile frame the target electron needs to transfer an increased momentum to the projectile electron in the mechanism proceeding through the electron-electron interaction. But this also means that the momentum transfer from the projectile electron to the target electron in the target frame is increased as well. Therefore, with increasing binding energy in the projectile the requirement for a visible signature of the internal correlation in the target ($p_{e_0} \gg q_e$) is increasingly difficult to satisfy.

Another reason for the discrepancies between theory and experiment could be higher-order effects. The longitudinal electron momentum spectra show that for the target electrons the PCI with the projectile electron is quite important. It is conceivable that for the projectile electrons the transverse momenta are more sensitive to the PCI than the longitudinal component, which would explain why the calculation reproduces the longitudinal spectrum better than the angular distribution of Fig. 5(b). Furthermore, other types of higher-order processes, e.g., those involving an interaction between the cores of both collision partners, may be important. To test the role of this interaction, in Fig. 6 $\phi_{e_t\text{-rec}}$ is plotted versus the angle between the recoil ion and the H^0 core $\phi_{H\text{-rec}}$. So far, the strongest correlation we have discussed is the one between each electron and its parent atom. Figure 6 shows that the correlation between the two cores is even stronger because there is more intensity near the vertical line with $\phi_{H\text{-rec}}=180°$ than near the horizontal line with $\phi_{e_t\text{-rec}}=180°$. Apparently, in the azimuthal plane a considerable momentum exchange during the collision occurs between the two cores.

Although the H^-+He system contains only six particles it is already too complex to discuss even qualitatively what impact higher-order effects may have on the angular distributions of Figs. 4–6. Comprehensive calculations, including a realistic potential for the H^- projectile as well as the various higher-order effects discussed in this paper, are currently not feasible.

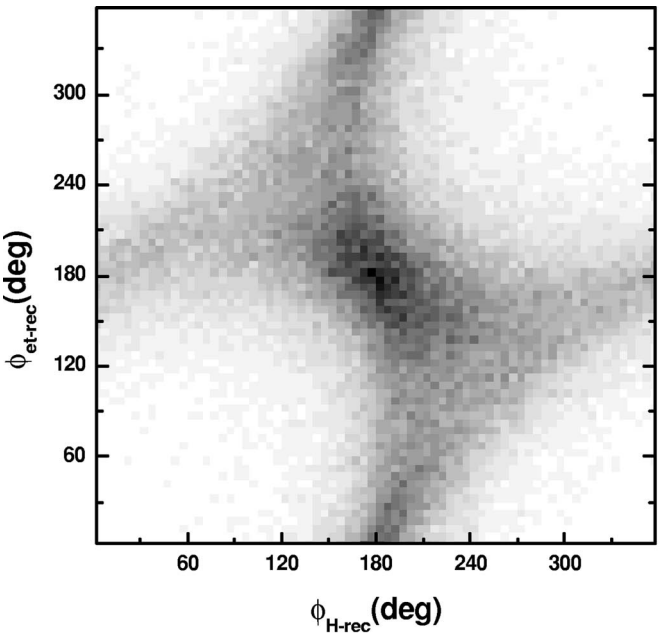

FIG. 6. The angle between the target electron and the He^+ recoil ion $\phi_{e_t\text{-rec}}$ versus the angle between the recoil ion and the H^0 core $\phi_{H\text{-rec}}$ in the azimuthal plane.

CONCLUSIONS

We have experimentally and theoretically studied mutual ionization in 200 keV H^-+He collisions. The longitudinal electron momentum spectra are consistent with a mechanism which proceeds through the electron-electron interaction dominating the ejection of both electrons. However, qualitative agreement with our calculations is only achieved if higher-order contributions in that interaction are accounted for. In the azimuthal angular distributions we find qualitative agreement for the target ionization between the measured data and our first-order calculation. For the projectile ionization, in contrast, large discrepancies are observed.

The poor agreement between our first-order calculation and the experimental data for the angular distributions in the azimuthal plane for the projectile electrons are probably partly due to higher-order effects. Those involving an interaction between the cores of both collision partners seem to be particularly strong. However, the most important factor appears to be a high sensitivity of these angular distributions to the momentum distribution in the initial projectile state. Given the small ionization potential of H^- one could easily be misguided to assume that the initial momentum distribution is relatively narrow. However, a better parameter relating to the momentum distribution is the average binding energy per electron, which is 10 times larger than the ionization potential. More importantly, for a short-range Yukawa potential the momentum distribution is significantly broader than for a long-range potential.

In order to shed more light on the dynamics of mutual ionization, experimental and theoretical studies of the FDCS are needed. These cross sections provide the most sensitive tests of theoretical models. Furthermore, the FDCS integrated over the momentum components of one electron and presented for the other electron (triply differential cross sections, TDCS) can be directly compared to FDCS for pure target ionization by charged particle impact. Such studies are presently in progress.

ACKNOWLEDGMENTS

One of the authors (M.S.) is grateful for the hospitality of the Max-Planck-Institut für Kernphysik in Heidelberg. We acknowledge the excellent work of the MPI accelerator staff for the prepararion of the ion beam. This work was supported by the Mercator Program of the Deutsche Forschungsgemeinschaft, the Gesellschaft für Schwerionenforschung, and the National Science Foundation under Grants Nos. PHY-0353532 and INT-0224943.

[1] W. Keever and E. Everhart, Phys. Rev. A **1**, 1083 (1970).
[2] M. E. Rudd, Y.-K. Kim, D. H. Madison, and J. W. Gallagher, Rev. Mod. Phys. **57**, 965 (1985).
[3] C. L. Cocke and R. E. Olson, Phys. Rep. **205**, 153 (1991).
[4] M. E. Rudd, Y.-K. Kim, D. H. Madison, and T. J. Gay, Rev. Mod. Phys. **64**, 441 (1992).
[5] N. Stolterfoht, R. D. Dubois, and R. D. Rivarola, *Electron Emission in Heavy Ion-Atom Collisions* (Springer-Verlag, Berlin, 1997).
[6] E. Y. Kamber, C. L. Cocke, S. Cheng, and S. L. Varghese, Phys. Rev. Lett. **60**, 2026 (1988).
[7] T. Vajnai, A. D. Gaus, J. A. Brand, W. Htwe, D. H. Madison, R. E. Olson, J. L. Peacher, and M. Schulz, Phys. Rev. Lett. **74**, 3588 (1995).
[8] M. Schulz, T. Vajnai, A. D. Gaus, W. Htwe, D. H. Madison, and R. E. Olson, Phys. Rev. A **54**, 2951 (1996).
[9] R. Dörner, V. Mergel, O. Jagutzki, L. Spielberger, J. Ullrich, R. Moshammer, and H. Schmidt-Böcking, Phys. Rep. **330**, 95 (2000).
[10] J. Ullrich, R. Moshammer, A. Dorn, R. Dörner, L. Schmidt, and H. Schmidt-Böcking, Rep. Prog. Phys. **66**, 1463 (2003).
[11] A. Gensmantel, J. Ullrich, R. Dörner, R. E. Olson, K. Ullmann, E. Forberich, S. Lencinas, and H. Schmidt-Böcking, Phys. Rev. A **45**, 4572 (1992).
[12] R. Moshammer, J. Ullrich, M. Unverzagt, W. Schmidt, P. Jardin, R. E. Olson, R. Mann, R. Dörner, V. Mergel, U. Buck, and H. Schmidt-Böcking, Phys. Rev. Lett. **73**, 3371 (1994).
[13] M. Schulz, R. Moshammer, D. H. Madison, R. E. Olson, P. Marchalant, C. T. Whelan, H. R. J. Walters, S. Jones, M. Foster, H. Kollmus, A. Cassimi, and J. Ullrich, J. Phys. B **34**, L305 (2001).
[14] M. Schulz, R. Moshammer, D. Fischer, H. Kollmus, D. H. Madison, S. Jones, and J. Ullrich, Nature (London) **422**, 48 (2003).
[15] M. Schulz, R. Moshammer, A. N. Perumal, and J. Ullrich, J. Phys. B **35**, L161 (2002).
[16] D. Fischer, R. Moshammer, M. Schulz, A. Voitkiv, and J. Ullrich, J. Phys. B **36**, 3555 (2003).
[17] A. Hasan, N. V. Maydanyuk, B. Fendler, A. Voitkiv, B. Najjari, and M. Schulz, J. Phys. B **37**, 1923 (2004).
[18] N. V. Maydanyuk, A. Hasan, M. Foster, B. Tooke, E. Nanni, D. H. Madison, and M. Schulz, Phys. Rev. Lett. **94**, 243201 (2005).
[19] A. B. Voitkiv, B. Najjari, R. Moshammer, M. Schulz, and J. Ullrich, J. Phys. B **37**, L365 (2004).
[20] M. Schulz, R. Moshammer, A. Voitkiv, B. Najjari, and J. Ullrich, Nucl. Instrum. Methods Phys. Res. B **235**, 296 (2005).
[21] D. Fischer, M. Schulz, R. Moshammer, and J. Ullrich, J. Phys. B **37**, 1103 (2004).
[22] M. Schulz, R. Moshammer, D. Fischer, and J. Ullrich, J. Phys. B **36**, L311 (2003).
[23] M. Schulz, R. Moshammer, D. Fischer, and J. Ullrich, J. Phys. B **37**, 4055 (2004).
[24] R. Moshammer, P. D. Fainstein, M. Schulz, W. Schmitt, H. Kollmus, R. Mann, S. Hagmann, and J. Ullrich, Phys. Rev. Lett. **83**, 4721 (1999).
[25] R. Moshammer, A. Perumal, M. Schulz, V. D. Rodríguez, H. Kollmus, R. Mann, S. Hagmann, and J. Ullrich, Phys. Rev. Lett. **87**, 223201 (2001).
[26] D. H. Madison, D. Fischer, M. Foster, M. Schulz, R. Moshammer, S. Jones, and J. Ullrich, Phys. Rev. Lett. **91**, 253201 (2003).
[27] R. E. Olson and J. Fiol, J. Phys. B **36**, L365 (2003).
[28] D. Fischer, R. Moshammer, A. Dorn, J. R. Crespo López-Urrutia, B. Feuerstein, C. Höhr, C. D. Schröter, S. Hagmann, H. Kollmus, R. Mann, B. Bapat, and J. Ullrich, Phys. Rev. Lett. **90**, 243201 (2003).
[29] M. Schulz, D. Fischer, R. Moshammer, and J. Ullrich, J. Phys. B **38**, 1363 (2005).
[30] R. Dörner, V. Mergel, R. Ali, U. Buck, C. L. Cocke, K. Froschauer, O. Jagutzki, S. Lencinas, W. E. Meyerhof, S. Nüttgens, R. E. Olson, H. Schmidt-Böcking, L. Spielberger, K. Tökesi, J. Ullrich, M. Unverzagt, and W. Wu, Phys. Rev. Lett. **72**, 3166 (1994).
[31] W. Wu, K. L. Wong, R. Ali, C. Y. Chen, C. L. Cocke, V. Frohne, J. P. Giese, M. Raphaelian, B. Walch, R. Dörner, V. Mergel, H. Schmidt-Böcking, and W. E. Meyerhof, Phys. Rev. Lett. **72**, 3170 (1994).
[32] H. Kollmus, R. Moshammer, R. E. Olson, S. Hagmann, M. Schulz, and J. Ullrich, Phys. Rev. Lett. **88**, 103202 (2002).
[33] J. S. Cohen and G. Fiorentini, Phys. Rev. A **33**, 1590 (1986).
[34] D. S. F. Crothers and J. F. McCann, J. Phys. B **16**, 3229 (1983).
[35] R. Moshammer, J. Ullrich, H. Kollmus, W. Schmitt, M. Unverzagt, H. Schmidt-Böcking, C. J. Wood, and R. E. Olson, Phys. Rev. A **56**, 1351 (1997).
[36] A. B. Voitkiv, B. Najjari, R. Moshammer, and J. Ullrich, Phys. Rev. A **65**, 032707 (2002).
[37] A. B. Voitkiv, B. Najjari, R. Moshammer, and J. Ullrich, J. Phys. B **37**, 4831 (2004).
[38] K. E. Banyard and J. C. Moore, J. Phys. B **10**, 2781 (1977).